Computer and Telecommunication Engineering (2023) Volume 1 Issue 1
doi: 10.54517/cte.v1i1.2327

ORIGINAL RESEARCH ARTICLE

Analyzing device-to-device communication performance with amplify-and-forward relaying amid co-channel interference

Huu Quy Tran

Faculty of Electronics Technology (FET), Industrial University of Ho Chi Minh City (IUH), Ho Chi Minh City 700000, Vietnam; tranquyhuu@iuh.edu.vn

ABSTRACT

Currently, the pressing issue of spectrum limitation, driven by the increasing demand for wireless communication services, has led to the challenge of co-channel interference (CCI) due to the reuse of frequencies in wireless networks. To address this, non-orthogonal multiple access (NOMA) has emerged as a solution. This report conducts a thorough evaluation of NOMA's system performance over independent and non-identical Rayleigh fading channels in device-to-device (D2D) communications networks, where CCI is significant. The analysis includes examining the probability density function (PDF) and cumulative distribution function (CDF) of the upper SINR threshold. Communication channels are defined as independent and non-identical Rayleigh fading channels, and probability expressions are formulated to assess system failure likelihood for two users. Additionally, Monte-Carlo simulations are conducted to validate the proposed theoretical mathematical expressions.

Keywords: amplified-and-forward; co-channel interference; outage probability; speed; throughput

1. Introduction

The device-to-device (D2D) communications network is a new application in 5th generation (5G) wireless networks. The exponential growth of data usage in mobile networks has prompted researchers and industry experts to explore innovative approaches distinct from traditional media. Among the recent methods that have garnered significant attention from researchers is D2D communication, which aims to alleviate mobile traffic congestion and leverage interoperability[1–4].

According to Gismalla et al.[5], the authors explored an inquiry into D2D communication concepts within the realm of 5G networks. This investigation encompasses the categorization of D2D communication as well as its diverse range of applications. The paper also evaluates the incorporation of D2D communication into the broader spectrum of contemporary technologies, such as cloud-based radio access networks, millimeter waves, the Internet of Things, visible light communication, ultra-dense networks, and unmanned aerial vehicles. It underscores the advantages of this integration within the context of 5G networks. Furthermore, the paper tackles the numerous challenges associated with D2D communication and proposes potential remedies, while also offering insights into future research trends. Importantly, the paragraph underscores that this review is

ARTICLE INFO
Received: 7 October 2023 | Accepted: 8 November 2023 | Available online: 19 December 2023

CITATION
Tran HQ. Analyzing device-to-device communication performance with amplify-and-forward relaying amid co-channel interference. *Computer and Telecommunication Engineering* 2023; 1(1): 2327. doi: 10.54517/cte.v1i1.2327

pioneering in the context of 6G, delineating essential prerequisites and anticipated research trajectories for the triumph of D2D communication in 6G networks.

The deployment of D2D networks in real-life scenarios necessitates addressing several crucial issues. For instance, when two users engage in direct D2D information exchange, they often contend with interference effects stemming from other nearby users. This interference can degrade service quality and result in reduced spectral efficiency. The impact of interference among users is commonly referred to as co-channel interference.

Co-channel interference represents a significant concern, not only in general collaborative wireless networks but also in D2D networks employing transient amplification techniques. Analyzing and mitigating co-channel interference is imperative when designing D2D network systems that leverage transient forwarding logic. This approach promotes efficient frequency channel reuse and maximizes spectral utilization[6,7]. Pei et al.[8] delved into the concept of mobile-edge computing offloading (MECO) and resource allocation within an energy-harvesting (EH) massive Internet of Things (mIoT) network supported by non-orthogonal multiple access (NOMA). The network encompasses machine-type communication devices (MTCDs) and roadside units (RSUs) randomly dispersed across a macrocell, incorporating a social trust model. The primary objective is to maximize the overall system data transmission rate while maintaining compliance with constraints related to transmit power, latency, quality of service (QoS), and energy consumption. To address this challenge, the problem is divided into three subproblems, which are solved using an iterative algorithm that includes processing mode selection, MTCD clustering, subchannel allocation, and power allocation. The article's simulations conclusively demonstrate the superior performance of the NOMA approach when compared to orthogonal multiple access (OMA). Tan et al.[9] devised a system for cell-free massive multiple-input multiple-output (MIMO) setups, focusing on energy-efficient layered division multiplexing (LDM) that supports both nonorthogonal multicast and unicast transmissions. Within this framework, numerous multi-antenna access points (APs) collaborate via a constrained-capacity backhaul network to collectively deliver multicast and unicast services to a large pool of user equipment (UEs). This design also facilitates concurrent information and power transfer.

The article provides a thorough analysis of how co-channel interference influences D2D networks when employing transient-forwarding techniques. It places particular emphasis on studying the ramifications of Rayleigh fading interference signals on all system users. The investigation encompasses various aspects, including outage probabilities, speed profiles, and system throughput. This analysis operates under the assumption that each user experiences a finite number of co-channel interferences.

We initiate by setting an upper limit for the signal-to-interference-plus-noise ratio (SINR) at the source user. Following that, we calculate the upper cumulative distribution function (CDF) of SINR. Using these outcomes, we develop expressions for assessing and evaluating probabilities related to magnitude, speed, and throughput.

Furthermore, in our endeavor to understand the impact of co-channel interference on D2D networks employing transient amplification techniques, the article provides simplified, approximate expressions for system warming probabilities.

2. System model

An illustration of the D2D communications network model considered in this work is shown in **Figure 1**. Two users, U_1 and U_2, aim to exchange information with each other via an amplify-and-forward (AF) relay, U_R. Each transmission period is divided into two phases: the multiple-access (MA) phase and the broadcasting (BC) phase. In the multiple-access phase, U_1 and U_2 simultaneously send their information messages to U_R.

In the broadcasting phase, the relay, U_R, normalizes the received signal based on its transmit energy constraint and broadcasts an amplified version of the received signal to U_1 and U_2. Transmissions are assumed to be performed over independent and non-identical Rayleigh fading channels.

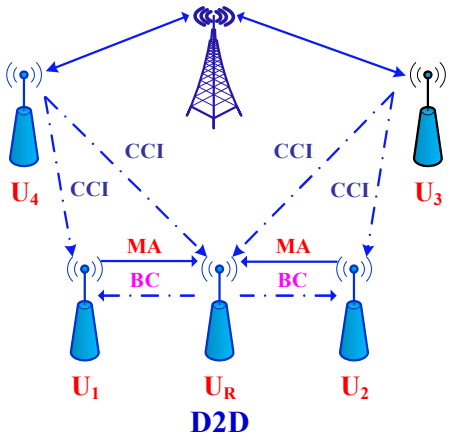

Figure 1. Two-way D2D forwarding network model that considers the co-channel interference effect.

For the sake of derivation simplicity and without loss of generality, we assume equal transmit energy for users U_1, U_2, and U_R, as well as equal variance for the additive white Gaussian noise (AWGN) at all three users. Furthermore, the article denotes and as the channel coefficients of the links $U_1 \rightarrow U_R$ and $U_2 \rightarrow U_R$, respectively, which are modeled as independent and non-identical Rayleigh random variables (RVs). This assumes that the channels are reciprocal, making the channel gains of links $U_1 \rightarrow U_R$ and $U_R \rightarrow U_i$, where i = 1, 2, identical. Lastly, this paper assumes that each user in the network is subject to a finite number of faded co-channel interfering signals from external sources.

Following the model described earlier, we can express the received signal during the multiple-access phase as Equation (1):

$$y_{U_R} = \sqrt{P_S} h X_{U_1} + \sqrt{P_S} g X_{U_2} + \sqrt{P_I} \sum_{j=1}^{L_{USR}} c_{U_{R,j}} d_{U_{R,j}} + N_{U_R} \tag{1}$$

Here are the components of the equation: X_{U_1} and X_{U_2} represent the unit-energy signals generated by users U_1 and U_2, respectively; $d_{U_{R,j}}$ denotes the signal from the j^{th} co-channel interferer's signal affecting U_R, and it is also assumed to have unit energy. The complex channel coefficients for the $U_1 \rightarrow U_R$ and $U_2 \rightarrow U_R$ links are represented as h and g, respectively. They possess power gains denoted as $|h|^2$ and $|g|^2$, which are assumed to follow exponential distributions with mean values $E[|h|^2] = \Omega_1$ and $E[|g|^2] = \Omega_2$, where $E[.]$ represents the expectation operation.

E_I represents the energy of the interference signal at USR; $c_{U_{R,j}}$ stands for the flat Rayleigh fading coefficient of the j^{th} interference channel; L_{U_R} epresents the total number of interference signals affecting the relay. Lastly, N_{U_R} represents the AWGN term at U_R.

In the broadcasting phase, the received signal at source U_1 is given by Equation (2):

$$y_{U_1} = Gh\sqrt{P_S} y_{U_R} + \sqrt{P_I} \sum_{k=1}^{L_{U_1}} c_{U_{1,k}} d_{U_{1,k}} + N_{U_{1,k}} \tag{2}$$

where G is the gain factor, $d_{U_{1,k}}$ is the k^{th} co-channel interferer's signal with unit energy affecting user U_1. $c_{U_{1,k}}$ is the flat Rayleigh fading coefficient of the k^{th} interference channel, L_{U_1} is the total number of interferers affecting user U_1 and N_{U_1} is the AWGN term at U_1.

By substituting the expression for y_{U_R} given in Equation (1) into Equation (2), we can express the signal received at user U_1 as Equation (3):

$$y_{U_1} = \mathrm{GP_S}h^2 X_{U_1} + \mathrm{GP_S hg X_{U_2}} + \mathrm{Gh}\sqrt{P_S}N_{U_R} + \mathrm{Gh}\sqrt{P_S}\sqrt{P_I}\sum_{\mathrm{j}=1}^{L_{U_R}} c_{U_{R,j}} d_{U_{R,j}} + \sqrt{P_I}\sum_{\mathrm{k}=1}^{L_{U_1}} c_{U_{1,k}} d_{U_{1,k}} + \mathrm{N}_{U_1} \tag{3}$$

In the AF relaying technique, the relay users are unable to distinguish between the source signal and any interference signals that may impact the transmission. This is because the amplification process occurs in the analog domain and involves a straightforward normalization of the total received power without additional processing. Consequently, implementing techniques like dirty paper coding and interference mitigation at the U_R becomes challenging. In our system, the amplification factor is expressed as Equation (4):

$$G = \sqrt{\frac{1}{P_S h^2 + P_S g^2 + P_I \sum_{j=1}^{L_{U_R}} c_{U_{R,j}}^2 + N_0}} \tag{4}$$

Since each source user knows its transmitted signal, it then cancels the self-interference term. Thus, the equivalent SINR at user U_1, denoted, can be written as in Equation (5).

Given that each source user has knowledge of its transmitted signal, it can effectively cancel out the self-interference term. Consequently, the equivalent SINR at user U_1, denoted as γ_{U_1}, can be expressed as shown in Equation (5).

$$\gamma_{U_1} = \frac{G^2 P_S^2 h^2 g^2}{G^2 h^2 P_S P_I \sum_{j=1}^{L_{U_R}} c_{U_{R,j}}^2 + P_I \sum_{k=1}^{L_{U_1}} c_{U_{1,k}}^2 + G^2 h^2 P_S N_0 + N_0} \tag{5}$$

To streamline the expression above, we introduce the notations $\gamma_S = P_S/N_0$ and $\gamma_I = P_I/N_0$. Subsequently, by substituting the value of G as provided in Equation (4) into Equation (5) and undertaking further intricate manipulations, we derive Equation (6):

$$\gamma_{U_1} = \frac{\frac{\gamma_S g^2}{1+\gamma_I \sum_{j=1}^{L_{U_R}} c_{U_{R,j}}^2} \times \frac{\gamma_S h^2}{1+\gamma_I \sum_{k=1}^{L_{U_1}} c_{U_{1,k}}^2}}{\frac{\gamma_S h^2}{1+\gamma_I \sum_{k=1}^{L_{U_1}} c_{U_{1,k}}^2} + \frac{\gamma_S g^2 + \gamma_S h^2}{1+\gamma_I \sum_{j=1}^{L_{USR}} c_{U_{R,j}}^2} + 1} \tag{6}$$

Likewise, it can be demonstrated in Equation (7):

$$\gamma_{U_2} = \frac{\frac{\gamma_S g^2}{\gamma_I \sum_{k=1}^{L_{U_2}} c_{U_{2,k}}^2} \times \frac{\gamma_S h^2}{\gamma_I \sum_{j=1}^{L_{U_R}} c_{U_{R,j}}^2}}{\frac{\gamma_S g^2}{\gamma_I \sum_{k=1}^{L_{U_2}} c_{U_{2,k}}^2} + \frac{\gamma_S g^2 + \gamma_S h^2}{\gamma_I \sum_{j=1}^{L_{U_R}} c_{U_{R,j}}^2} + 1} \tag{7}$$

Here, $c_{U_{2,k}}$ represents the flat Rayleigh fading coefficient of the k^{th} interference channel affecting user U_2 and L_{U_2} signifies the total count of co-channel interference signals impacting U_2.

3. Performance analysis of D2D communication using amplify-and-forward technique

In this section, an examination of the statistical properties of the equivalent SINR will be conducted. Furthermore, a lower bound on the error and outage probabilities for device-to-device communication utilizing the AF technique will be established. Additionally, significant observations derived from the analysis will be presented.

3.1. CDF of the equivalent SINRs

To facilitate a more mathematically tractable performance analysis, we aim to express Equation (6) in a simplified form. To accomplish this, we introduce stringent upper bounds on the equivalent SINRs in Equations (8) and (9):

$$\gamma_{U_1} \leq \gamma_{U_1}^{up} = min\left(\frac{\gamma_S g^2}{I_{U_R} + I_{U_1} + 2}, \frac{\gamma_S h^2}{I_{U_1} + 1}\right) \tag{8}$$

$$\gamma_{U_2} \leq \gamma_{U_2}^{up} = min\left(\frac{\gamma_S h^2}{I_{U_R} + I_{U_2} + 2}, \frac{\gamma_S g^2}{I_{U_2} + 1}\right) \tag{9}$$

where $I_{U_R} = \gamma_I \sum_{j=1}^{L_{U_R}} c_{U_R,j}^2$, $I_{U_1} = \gamma_I \sum_{k=1}^{L_{U_1}} c_{U_1,k}^2$ and $I_{U_2} = \gamma_I \sum_{k=1}^{L_{U_2}} c_{U_2,k}^2$, denote the total co-channel interference affecting users U_2, U_R and U_2, respectively. The appendix demonstrates that the CDF of the upper-bound SINR, $\gamma_{U_1}^{up}$, can be expressed as follows:

$$F_{\gamma_{U_1}}(\gamma) \geq F_{\gamma_{U_1}^{up}}(\gamma) = 1 - \left(\frac{\frac{\gamma_S \Omega_h}{\gamma_I \Omega_c}}{\gamma + \frac{\gamma_S \Omega_h}{\gamma_I \Omega_c}}\right)^{L_{U_1}} \left(\frac{\frac{\gamma_S \Omega_g}{\gamma_I \Omega_c}}{\gamma + \frac{\gamma_S \Omega_g}{\gamma_I \Omega_c}}\right)^{L_{U_R}+L_{U_1}} exp\left(-\gamma\left[\frac{2}{\gamma_S \Omega_g} + \frac{1}{\gamma_S \Omega_h}\right]\right) \tag{10}$$

where $F_{\gamma_{U_1}}(\gamma)$ is the exact CDF of γ_{U_1}, $\Omega_h = E(h^2)$, $\Omega_g = E(g^2)$, $\Omega_c = E\left(c_{U_R,j}^2\right) = E\left(c_{U_1,k}^2\right)$, $\left(j = 1, \ldots, L_{U_R};\ k = 1, \ldots, L_{U_1}\right)$ and $E(.)$ represents the expectation operator. It is worth mentioning that when dealing with identical channels and the same number of interference sources, denoted as $\Omega_h = \Omega_g = \Omega$ and $L_{U_R} = L_{U_2} = L$, respectively, Equation (10) simplifies to Equation (11):

$$F_{\gamma_{U_1}^{up}}(\gamma) = 1 - \left(\frac{\frac{\gamma_S \Omega}{\gamma_I \Omega_c}}{\gamma + \frac{\gamma_S \Omega}{\gamma_I \Omega_c}}\right)^{3L} exp\left(-\gamma\left[\frac{3}{\gamma_S \Omega}\right]\right) \tag{11}$$

Moreover, in the scenario where there is no interference, i.e., when $L_{U_R} = L_{U_1} = 0$, the CDF of $\gamma_{U_1}^{up}$ can be significantly simplified to Equation (12):

$$F_{\gamma_{U_1}^{up}}(\gamma) = 1 - exp\left(-\gamma\left[\frac{2}{\gamma_S \Omega_g} + \frac{1}{\gamma_S \Omega_h}\right]\right) \tag{12}$$

Applying a similar approach to the one mentioned above, the CDF of the SINR at user U_2 can be expressed as Equation (13):

$$F_{\gamma_2^{up}}(\gamma) = 1 - \left(\frac{\frac{\gamma_S \Omega_h}{\gamma_I \Omega_c}}{\gamma + \frac{\gamma_S \Omega_h}{\gamma_I \Omega_c}}\right)^{L_{U_R}+L_{U_2}} \left(\frac{\frac{\gamma_S \Omega_g}{\gamma_I \Omega_c}}{\gamma + \frac{\gamma_S \Omega_g}{\gamma_I \Omega_c}}\right)^{L_{U_2}} exp\left(-\gamma\left[\frac{1}{\gamma_S \Omega_g} + \frac{2}{\gamma_S \Omega_h}\right]\right) \tag{13}$$

The outage probability is defined as the probability that the channel mutual information falls below the required rate $r$bits/sec/Hz. Hence, we can formulate the outage probability as Equation (14):

$$P_{U_i}(out) = Pr\left(R_{U_i} \le r\right) = Pr\left(\gamma_{U_i} \le \gamma_T\right), i = 1,2 \tag{14}$$

where $\gamma_T = 2^{2r} - 1$. Consequently, $P_{U_i}(out)$ is essentially the CDF of $\gamma_{U_i}^{up}, i = 1,2$ evaluated at $2^{2r} - 1$.

3.2. Asymptotic analysis

While the expressions obtained in the previous section allow for the numerical evaluation of the system's performance and are not computationally intensive, they do not provide intuitive insights into the effects of the system parameters.

To address this, we now introduce new closed-form expressions for $F_{\gamma_{U_1}^{up}}(\gamma)$ in simpler, more understandable forms.

The same approach can be applied to obtain results for user U_2. Therefore, by employing Taylor's series, $F_{\gamma_{U_1}^{up}}(\gamma)$ can be expressed as Equation (15):

$$F_{\gamma_{U_1}^{up}}(\gamma) \to \left[\frac{1}{\gamma_S \Omega_{h}}\left(1 + L_{U_1}\gamma_I\Omega_c\right) + \frac{1}{\gamma_S\Omega_g}\left(2 + \left(L_{U_R} + L_{U_1}\right)\gamma_I\Omega_c\right)\right]\gamma + o(\gamma) \tag{15}$$

Here, $o(\gamma)$ represents higher-order terms. It's worth recalling that $P_{U_1}(out)$ can be expressed as $P_{U_1}(out) = F_{\gamma_{U_1}^{up}}(2^{2r} - 1)$.

The instantaneous maximum rates for users U_1 and U_2 are determined by Equation (16):

$$R_{U_i} = \frac{1}{2} log_2\left(1 + \gamma_{U_i}^{up}\right), i = 1,2 \tag{16}$$

The 1/2 factor accounts for the two time slots required for data transmission, one in the multiple-access phase and the other in the broadcasting phase.

3.3. Achievable rate

According to Shannon's definition, the key performance metric of the system is the achieved speed, as it offers insights into the maximum achievable transfer rates and the system's error correction capabilities. The achieved speed can be determined as Equation (17):

$$R = \frac{1}{2}\left[E\left\{log_2\left(1 + \gamma_{U_1}^{up}\right)\right\} + E\left\{log_2\left(1 + \gamma_{U_2}^{up}\right)\right\}\right] \tag{17}$$

The upper bound on speed is as Equation (18):

$$R \le \frac{1}{2}\left[log_2\left(1 + E\{\gamma_{U_1}^{up}\}\right) + log_2\left(1 + E\{\gamma_{U_2}^{up}\}\right)\right] \tag{18}$$

Here, the term $E\left\{\gamma_{U_i}^{up}\right\}$, where *i* equals 1 or 2, is defined as Equation (19):

$$E\left\{\gamma_{U_i}^{up}\right\} = \int_0^\infty \left(1 - F_{\gamma_{U_i}^{up}}(x)\right) dx \tag{19}$$

3.4. The throughput

The throughput of the D2D communications network using the AF technique can be expressed as τ, where in Equation (20):

$$\tau = \frac{1}{2}(1 - P_{out})R \tag{20}$$

4. Numerical results and discussion

In this section, numerical results are presented to substantiate the analysis developed in the preceding sections. Additionally, the impact of interference on the performance of D2D communication employing the AF technique is scrutinized. It is assumed that the distance between the network's terminals follows a uniform distribution.

Figure 2 displays the error probability performance for D2D communication in AF technique networks with different numbers of interferers. The outage probabilities depicted in the graph are obtained from simulations and are contrasted with the respective lower bounds. Moreover, **Figure 2** incorporates the asymptotic outcomes for the outage probabilities, as derived from the expressions in Equation (15). To provide a benchmark, we've also included the performance of the interference-free network. It is noteworthy that the derived lower bound closely matches the exact results, even in the low P_S/N_0 region. The asymptotical expressions also provide an excellent match in the moderate-to-high P_S/N_0 region $(P_S/N_0 \geq 9dB)$. Moreover, in the low and medium ranges of P_S/N_0, increasing P_S/N_0 improves the outage probability performance since the dominant noise in these regions is AWGN. On the other hand, error floors appear at high P_S/N_0 due to the presence of the cochannel interference which is independent of P_S/N_0.

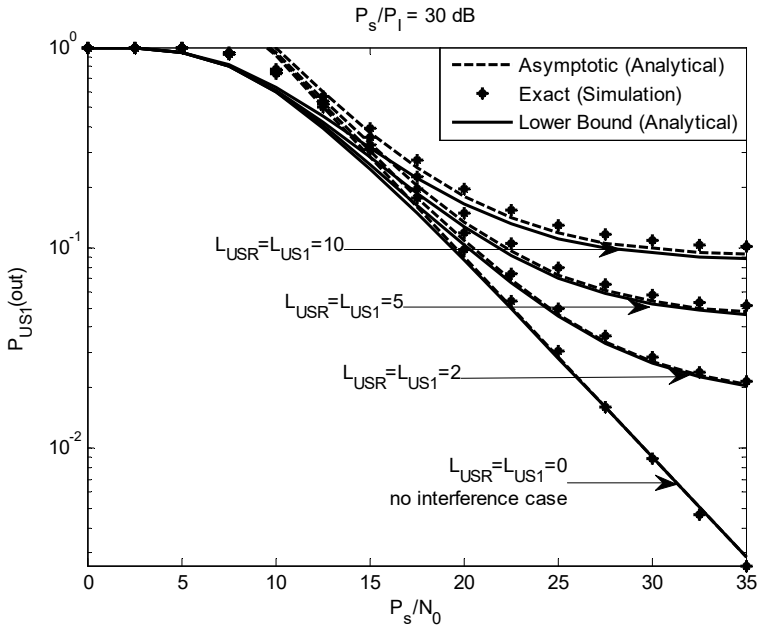

Figure 2. Outage probability in co-channel interference for D2D communication using the AF technique with different numbers of co-channel interference signals.

Figure 3 illustrates the achievable rate in D2D communication using the AF technique, considering the impact of co-channel interference. It is evident from **Figure 3** that as the number of interferers increases, the system speed decreases. System stability improves as P_S/N_0 increases.

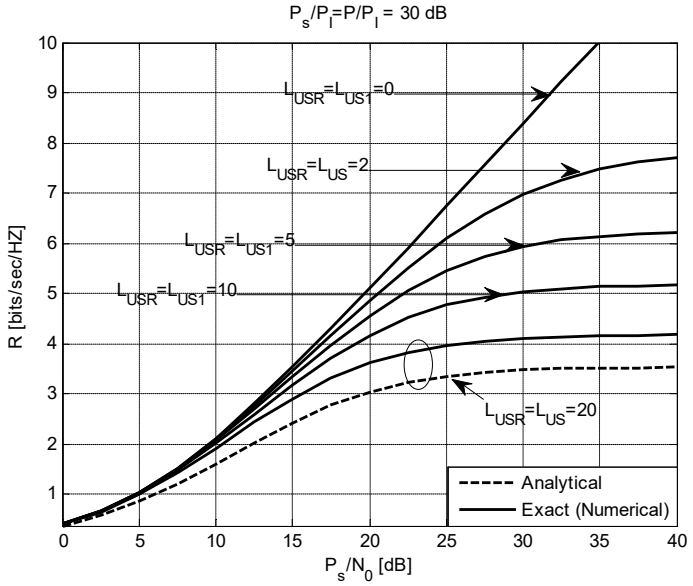

Figure 3. Achievable Rate in co-channel interference on D2D communication using AF technique with different numbers of co-channel interference signals.

5. Conclusion

This paper delves into the examination of how co-channel interference affects the performance of D2D communication when utilizing the AF technique. The study assumes that the desired signal undergoes independent Rayleigh fading. Furthermore, it takes into account an arbitrary count of independent interference signals, each experiencing Rayleigh fading with equivalent power and fading characteristics.

The derived expressions for outage probabilities, based on a tight lower bound on the effective SINR, have demonstrated a close match with simulation results. These expressions are applicable to scenarios with varying numbers of interferers and support any modulation scheme.

The article has evaluated the throughput and achievable rate of co-channel interference in D2D communication. Future research in this context could explore interference cancellation techniques that address the presented performance limitations and consider the impact of practical time-varying channels.

Conflict of interest

The author declares no conflict of interest.

References

1. Andreev S, Pyattaev A, Johnsson K, et al. Cellular traffic offloading onto network-assisted device-to-device connections. *IEEE Communications Magazine* 2014; 52(4): 20–31. doi: 10.1109/MCOM.2014.6807943
2. Wei L, Hu RQ, Qian Y, Wu G. Enable device-to-device communications underlaying cellular networks: Challenges and research aspects. *IEEE Communications Magazine* 2014; 52(6): 90–96. doi: 10.1109/MCOM.2014.6829950
3. Erturk MC, Mukherjee S, Ishii H, Arslan H. Distributions of transmit power and SINR in device-to-device networks. *IEEE Communications Letters* 2013; 17(2): 273–276. doi: 10.1109/LCOMM.2012.122012.121632
4. Lee N, Lin X, Andrews JG, Heath RW. Power control for D2D underlaid cellular networks: Modeling, algorithms, and analysis. *IEEE Journal on Selected Areas in Communications* 2014; 33(1): 1–13. doi: 10.1109/JSAC.2014.2369612
5. Gismalla MS, Azmi AI, Salim MR, et al. Survey on device to device (D2D) communication for 5GB/6G networks: Concept, applications, challenges, and future directions. *IEEE Access* 2022; 10: 30792–30821. doi: 10.1109/ACCESS.2022.3160215

6. Radaydeh RM. On the bandwidth efficiency of D2D link adaptation under co-channel interference. In: Proceedings of the 2021 IEEE 12th Annual Information Technology, Electronics and Mobile Communication Conference (IEMCON); 27–30 October 2021; Vancouver, BC, Canada. pp. 976–981. doi: 10.1109/IEMCON53756.2021.9623109
7. Radaydeh RM. On the performance of imperfect simultaneous D2D association under co-channel interference. In: Proceedings of the 2022 IEEE Wireless Communications and Networking Conference (WCNC); 10–13 April 2022; Austin, TX, USA. pp. 2005–2010. doi: 10.1109/WCNC51071.2022.9771692
8. Pei X, Duan W, Wen M, et al. Socially aware joint resource allocation and computation offloading in NOMA-aided energy-harvesting massive IoT. *IEEE Internet of Things Journal* 2020; 8(7): 5240–5249. doi: 10.1109/JIOT.2020.3034380
9. Tan F, Wu P, Wu YC, Xia M. Energy-efficient non-orthogonal multicast and unicast transmission of cell-free massive MIMO systems with SWIPT. *IEEE Journal on Selected Areas in Communications* 2020; 39(4): 949–968. doi: 10.1109/JSAC.2020.3020110
10. Papoulis A, Pillai SU. *Random Variables and Stochastic Processes*, 4th ed. McGraw-Hill Europe; 2002. 852p.
11. Aalo VA, Zhang J. Performance analysis of maximal ratio combining in the presence of multiple equal-power cochannel interferers in a Nakagami fading channel. *IEEE Transactions on Vehicular Technology* 2001; 50(2): 497–503. doi: 10.1109/25.923061

Appendix

Transform Equation (6) in Equation (21):

$$\gamma_{U_1}=\frac{\frac{\gamma_S g^2}{1+I_{U_R}}\times\frac{\gamma_S h^2}{1+I_{U_1}}}{\frac{\gamma_S h^2}{1+I_{U_1}}+\frac{\gamma_S g^2+\gamma_S h^2}{1+I_{U_R}}+1}\cong\frac{\frac{\gamma_S g^2}{1+I_{U_R}}\times\frac{\gamma_S h^2}{1+I_{U_1}}}{\frac{\gamma_S h^2}{1+I_{U_1}}+\frac{\gamma_S g^2+\gamma_S h^2}{1+I_{U_R}}}=\frac{\frac{\gamma_S g^2}{2+I_{U_R}+I_{U_1}}\times\frac{\gamma_S h^2}{1+I_{U_1}}\times\frac{2+I_R+Is_1}{1+I_{U_R}}}{\frac{\gamma_S h^2(1+I_{U_R})+(1+I_{U_1})(\gamma_S g^2+\gamma_S h^2)}{(1+I_{U_1})(1+I_{U_R})}}=\frac{\frac{\gamma_S g^2}{2+I_{U_R}+I_{U_1}}\times\frac{\gamma_S h^2}{1+I_{U_1}}\times\frac{2+I_{U_R}+I_{U_1}}{1+I_{U_R}}}{\frac{\gamma_S h^2(2+I_{U_R}+I_{U_1})+(1+I_{U_1})\gamma_S g^2}{(1+I_{U_1})(1+I_{U_R})}}=\frac{\frac{\gamma_S g^2}{2+I_{U_R}+I_{U_1}}\times\frac{\gamma_S h^2}{1+I_{U_1}}}{\frac{\gamma_S g^2}{2+I_{U_R}+I_{U_1}}+\frac{\gamma_S h^2}{1+I_{U_1}}} \tag{21}$$

By applying the strict upper bound theorem to the equivalent SINR, we obtain Equation (22):

$$\gamma_{U_1}^{up}=min(\frac{\gamma_S g^2}{I_{U_R}+I_{U_1}+2},\frac{\gamma_S h^2}{I_{U_1}+1})=min\left(\gamma_g^{U_1},\gamma_h^{U_1}\right) \tag{22}$$

where $\gamma_g^{U_1}=\frac{\gamma_S g^2}{(I_{U_R}+I_{U_1}+2)}$ and $\gamma_g^{U_1}=\frac{\gamma_S h^2}{(I_{U_1}+1)}$. We are aware that the CDF of $\gamma_{U_1}^{up}$ can be expressed as a function of the CDFs of $\gamma_g^{U_1}$ and $\gamma_h^{U_1}$, denoted as $F_{\gamma_{U_1}^{up}}(\gamma)=1-P_r\left(\gamma_h^{U_1}>\gamma,\gamma_g^{U_1}>\gamma\right)$ $F_{\gamma_{U_1}^{up}}(\gamma)\approx 1-\left(1-F_{\gamma_h^{U_1}}(\gamma)\right)\left(1-F_{\gamma_g^{U_1}}(\gamma)\right)$, respectively.

Generally, $\gamma_g^{U_1}$ and $\gamma_h^{U_1}$ are not independent. However, during a Monte Carlo simulation, we observed that as long as $\frac{\gamma_S}{\gamma_I}>1$, the percentage error remains below 10^{-3} across the entire SNR region. Therefore, this assumption can be confidently applied for practical purposes. Now, recall that $\gamma_S g^2$ and $\gamma_S h^2$ are exponentially distributed random variables (RVs) according to $f_{\gamma_S g^2}(x)=\left(\frac{1}{\gamma_S\Omega_g}\right)exp\left(\frac{-x}{\gamma_S\Omega_g}\right)$ and $f_{\gamma_S h^2}(x)=\left(\frac{1}{\gamma_S\Omega_h}\right)exp\left(\frac{-x}{\gamma_S\Omega_h}\right)$, with parameters $\Omega_g=E(g^2)$ and $\Omega_h=E(h^2)$.

Also, $I_{U_R}=\gamma_I\sum_{j=1}^{L_{U_R}}c_{U_R,j}^2$ and $I_{U_1}=\gamma_I\sum_{k=1}^{L_{U_1}}c_{U_1,k}^2$ represent the total interference signals affecting users U_R and U_1, respectively. Then, the PDFs of I_{U_R} and I_{U_1} can be expressed as per reference[10]. $f_{I_{U_R}}(x)=\left(\frac{1}{\gamma_I\Omega_c}\right)^{L_{U_R}}\frac{x^{L_{U_R}-1}}{(L_{U_R}-1)!}exp\left(-\frac{x}{\gamma_I\Omega_c}\right)$ and $f_{I_{U_1}}(x)=\left(\frac{1}{\gamma_I\Omega_c}\right)^{L_{U_1}}\frac{x^{L_{U_1}-1}}{(L_{U_1}-1)!}exp\left(-\frac{x}{\gamma_I\Omega_c}\right)$, where $\Omega_c=E\left(c_{U_R,j}^2\right)=E\left(c_{U_1,k}^2\right)$, $j=1,\ldots,L_{U_R};\ k=1,\ldots,L_{U_1}$

Therefore, with the assistance of reference[11], $F_{\gamma_h^{U_1}}(\gamma)$ can be expressed as Equation (23):

$$F_{\gamma_h^{U_1}}(\gamma)=1-\left(\frac{\frac{\gamma_S\Omega_h}{\gamma_I\Omega_c}}{\gamma+\frac{\gamma_S\Omega_h}{\gamma_I\Omega_c}}\right)^{L_{U_1}}exp\left(\frac{-\gamma}{\gamma_S\Omega_h}\right) \tag{23}$$

Now, let's consider the statistics of $\gamma_g^{U_1}$, specifically, the PDF and CDF of $\gamma_g^{U_1}$. These can be determined as follows: First, the PDF of $I_{U_R}+I_{U_1}$ can be expressed using[10], where $f_{I_{U_R}+I_{U_1}}(x)=f_{I_{U_R}}(x)*f_{I_{U_1}}(x)=\int_x^\infty f_{I_{U_R}}(y)\,f_{I_{U_1}}(x-y)dy\ (a)$. Here, * denotes the convolutional operation. After solving the integration in (a), $f_{I_{U_R}+I_{U_1}}(x)$ can be expressed in a closed form as Equation (24):

$$f_{I_{U_R}+I_{U_1}}(x)=\frac{\left(\frac{1}{\gamma_I\Omega_c}\right)^{L_{U_R}+L_{U_1}}x^{L_{U_R}+L_{U_1}-1}}{\left(L_{U_R}+L_{U_1}-1\right)!}exp\left(-\frac{x}{\gamma_I\Omega_c}\right) \tag{24}$$

Subsequently, with the assistance of research by Aalo and Zhang [11], the CDF of $\gamma_g^{U_1}$, denoted as $F_{\gamma_g^{U_1}}(\gamma)$, can be expressed as Equation (25):

$$F_{\gamma_{U_1}^{up}}(\gamma) = 1 - \left(\frac{\frac{\gamma_S \Omega_g}{\gamma_I \Omega_c}}{\gamma + \frac{\gamma_S \Omega_g}{\gamma_I \Omega_c}} \right)^{L_{U_R} + L_{U_1}} exp\left(\frac{-2\gamma}{\gamma_S \Omega_g} \right) \tag{25}$$

The CDF of $\gamma_{U_1}^{up}$ is obtained as Equation (26):

$$F_{\gamma_{U_1}^{up}}(\gamma) = 1 - \left(\frac{\frac{\gamma_S \Omega_g}{\gamma_I \Omega_c}}{\gamma + \frac{\gamma_S \Omega_g}{\gamma_I \Omega_c}} \right)^{L_{U_1}} \left(\frac{\frac{\gamma_S \Omega_g}{\gamma_I \Omega_c}}{\gamma + \frac{\gamma_S \Omega_g}{\gamma_I \Omega_c}} \right)^{L_{U_R} + L_{U_1}} exp\left(-\gamma \left[\frac{2}{\gamma_S \Omega_g} + \frac{1}{\gamma_S \Omega_h} \right] \right) \tag{26}$$